



**HAL**  
open science

## The Reading Palaeofire Database: an expanded global resource to document changes in fire regimes from sedimentary charcoal records

Sandy P. Harrison, Roberto Villegas-Diaz, Esmeralda Cruz-Silva, Daniel Gallagher, David Kesner, Paul Lincoln, Yicheng Shen, Luke Sweeney, Daniele Colombaroli, Adam Ali, et al.

### ► To cite this version:

Sandy P. Harrison, Roberto Villegas-Diaz, Esmeralda Cruz-Silva, Daniel Gallagher, David Kesner, et al.. The Reading Palaeofire Database: an expanded global resource to document changes in fire regimes from sedimentary charcoal records. *Earth System Science Data*, 2022, 14, pp.1109-1124. 10.5194/essd-14-1109-2022 . insu-03678657

**HAL Id: insu-03678657**

**<https://insu.hal.science/insu-03678657>**

Submitted on 25 May 2022

**HAL** is a multi-disciplinary open access archive for the deposit and dissemination of scientific research documents, whether they are published or not. The documents may come from teaching and research institutions in France or abroad, or from public or private research centers.

L'archive ouverte pluridisciplinaire **HAL**, est destinée au dépôt et à la diffusion de documents scientifiques de niveau recherche, publiés ou non, émanant des établissements d'enseignement et de recherche français ou étrangers, des laboratoires publics ou privés.



Distributed under a Creative Commons Attribution 4.0 International License



## The Reading Palaeofire Database: an expanded global resource to document changes in fire regimes from sedimentary charcoal records

Sandy P. Harrison<sup>1,2</sup>, Roberto Villegas-Díaz<sup>1</sup>, Esmeralda Cruz-Silva<sup>1</sup>, Daniel Gallagher<sup>2,3</sup>, David Kesner<sup>1,2</sup>, Paul Lincoln<sup>1,2</sup>, Yicheng Shen<sup>1</sup>, Luke Sweeney<sup>1,2</sup>, Daniele Colombaroli<sup>2,3</sup>, Adam Ali<sup>4</sup>, Chéïma Barhoumi<sup>5</sup>, Yves Bergeron<sup>6,7</sup>, Tatiana Blyakharchuk<sup>8</sup>, Přemysl Bobek<sup>9</sup>, Richard Bradshaw<sup>10</sup>, Jennifer L. Clear<sup>11</sup>, Sambor Czerwiński<sup>12</sup>, Anne-Laure Daniau<sup>13</sup>, John Dodson<sup>14,15</sup>, Kevin J. Edwards<sup>16,17,18,19</sup>, Mary E. Edwards<sup>20</sup>, Angelica Feurdean<sup>21</sup>, David Foster<sup>22</sup>, Konrad Gajewski<sup>23</sup>, Mariusz Gałka<sup>24</sup>, Michelle Garneau<sup>25</sup>, Thomas Giesecke<sup>26</sup>, Graciela Gil Romera<sup>27,28</sup>, Martin P. Girardin<sup>29</sup>, Dana Hoefler<sup>30</sup>, Kangyou Huang<sup>31</sup>, Jun Inoue<sup>32</sup>, Eva Jamrichová<sup>9</sup>, Nauris Jasiunas<sup>33</sup>, Wenying Jiang<sup>34</sup>, Gonzalo Jiménez-Moreno<sup>35</sup>, Monika Karpińska-Kołodziej<sup>12</sup>, Piotr Kołodziej<sup>12</sup>, Niina Kuosmanen<sup>36</sup>, Mariusz Lamentowicz<sup>37</sup>, Martin Lavoie<sup>38</sup>, Fang Li<sup>39</sup>, Jianyong Li<sup>40</sup>, Olga Lisitsyna<sup>41,42</sup>, José Antonio López-Sáez<sup>43</sup>, Reyes Luelmo-Lautenschlaeger<sup>43</sup>, Gabriel Magnan<sup>25</sup>, Eniko Katalin Magyari<sup>44</sup>, Alekss Maksims<sup>45</sup>, Katarzyna Marcisz<sup>12</sup>, Elena Marinova<sup>46</sup>, Jenn Marlon<sup>47</sup>, Scott Mensing<sup>48</sup>, Joanna Mirosław-Grabowska<sup>49</sup>, Wyatt Oswald<sup>22,50</sup>, Sebastián Pérez-Díaz<sup>51</sup>, Ramón Pérez-Obiol<sup>52</sup>, Sanna Piilo<sup>53</sup>, Anneli Poska<sup>41,54</sup>, Xiaoguang Qin<sup>34</sup>, Cécile C. Remy<sup>55</sup>, Pierre J. H. Richard<sup>56</sup>, Sakari Salonen<sup>36</sup>, Naoko Sasaki<sup>57</sup>, Hieke Schneider<sup>58</sup>, William Shotyk<sup>59</sup>, Migle Stancikaite<sup>60</sup>, Dace Šteinberga<sup>45</sup>, Normunds Stivrins<sup>33,41,61</sup>, Hikaru Takahara<sup>62</sup>, Zhihai Tan<sup>63</sup>, Liva Trasune<sup>33,36</sup>, Charles E. Umbanhowar<sup>64,65</sup>, Minna Väliranta<sup>53</sup>, Jüri Vassiljev<sup>41</sup>, Xiayun Xiao<sup>66</sup>, Qinghai Xu<sup>67</sup>, Xin Xu<sup>39</sup>, Edyta Zawisza<sup>49</sup>, Yan Zhao<sup>68</sup>, Zheng Zhou<sup>31</sup>, and Jordan Paillard<sup>56</sup>

<sup>1</sup>School of Archaeology, Geography and Environmental Science, University of Reading, Whiteknights, Reading, RG6 6AH, UK

<sup>2</sup>Leverhulme Centre for Wildfires, Environment and Society, Imperial College London, South Kensington, London, SW7 2BW, UK

<sup>3</sup>Department of Geography, Royal Holloway, University of London, Egham, TW20 0SS, UK

<sup>4</sup>Institut des Sciences de l'Évolution de Montpellier (CNRS, IRD, EPHE), Université de Montpellier, 34090 Montpellier, France

<sup>5</sup>Department of Palynology and Climate Dynamics, Albrecht-von-Haller-Institute for Plant Sciences, University of Göttingen, Untere Karspüle 2, 37073 Göttingen, Germany

<sup>6</sup>Forest Research Institute (IRF), Université du Québec en Abitibi-Témiscamingue (UQAT), Rouyn-Noranda, QC, J9X 5E4, Canada

<sup>7</sup>Department of Biological Sciences, Université du Québec à Montréal (UQAM), Montréal, QC, H3C 3P8, Canada

<sup>8</sup>Institute of Monitoring of Climatic and Ecological Systems of Siberian branch of the Russian Academy of Sciences (IMCES SB RAS), 634055, Tomsk, Russia

<sup>9</sup>Institute of Botany, Czech Academy of Sciences, Lidická 25/27, 602 00 Brno, Czech Republic

<sup>10</sup>Geography and Planning, University of Liverpool, Liverpool, L69 7ZT, UK

<sup>11</sup>Department of Geography and Environmental Science, Liverpool Hope University, Taggart Street, Childwall, Liverpool, L16 9JD, UK

<sup>12</sup>Climate Change Ecology Research Unit, Faculty of Geographical and Geological Sciences, Adam Mickiewicz University Poznań, Bogumiła Krygowskiego 10, 61-680 Poznań, Poland

- <sup>13</sup>Environnements et Paléoenvironnements Océaniques et Continentaux (EPOC), Unité Mixte de Recherche (UMR) 5805, Centre National de la Recherche Scientifique (CNRS), Université de Bordeaux, 33615 Pessac, France
- <sup>14</sup>Institute of Earth Environment, Chinese Academy of Sciences, Keji 1st Rd, Yanta District, Xi'an, Shaanxi, 710061, Shaanxi Province, China
- <sup>15</sup>School of Earth, Atmospheric and Life Sciences, University of Wollongong, Wollongong, NSW 2500, Australia
- <sup>16</sup>Department of Geography and Environment, University of Aberdeen, Aberdeen, AB24 3UX, UK
- <sup>17</sup>Department of Archaeology, University of Aberdeen, AB24 3UX, UK
- <sup>18</sup>McDonald Institute for Archaeological Research, University of Cambridge, Cambridge, CB2 1TN, UK
- <sup>19</sup>Scott Polar Research Institute, University of Cambridge, Cambridge, CB2 1TN, UK
- <sup>20</sup>School of Geography and Environmental Science, University of Southampton, Southampton, SO17 1BJ, UK
- <sup>21</sup>Institute of Physical Geography, Goethe University Frankfurt, Altenhöferallee 1, 60438 Frankfurt am Main, Germany
- <sup>22</sup>Harvard Forest, Harvard University, Petersham, MA 01366, USA
- <sup>23</sup>Département de Géographie, Environnement et Géomatique, Université d'Ottawa, Ottawa, ON, K1N 6N5, Canada
- <sup>24</sup>Department of Biogeography, Paleocology and Nature Protection, Faculty of Biology and Environmental Protection, University of Lodz, 1/3 Banacha St., 90-237 Łódź, Poland
- <sup>25</sup>Geotop, Université du Québec à Montréal, Montréal, QC, H2X 3Y7, Canada
- <sup>26</sup>Department of Physical Geography, Faculty of Geosciences, Utrecht University, 2584 CS Utrecht, the Netherlands
- <sup>27</sup>Instituto Pirenaico de Ecología – CSIC, Avda. Montañana 1005, 50059 Zaragoza, Spain
- <sup>28</sup>Plant Ecology and Geobotany, Philipps University of Marburg, Karl-Von-Frisch-Straße 8, 35037 Marburg, Germany
- <sup>29</sup>Laurentian Forestry Centre, Canadian Forest Service, Natural Resources Canada, Québec City, QC, G1V V4C, Canada
- <sup>30</sup>Senckenberg Research Station of Quaternary Palaeontology, Am Jakobskirchhof 4, 99423 Weimar, Germany
- <sup>31</sup>School of Earth Sciences and Engineering, Sun Yat-sen University, Zhuhai 519082, China
- <sup>32</sup>Department of Geosciences, Graduate School of Science, Osaka City University, Osaka 558-8585, Japan
- <sup>33</sup>Department of Geography, University of Latvia, Jelgavas iela 1, Riga, 1004, Latvia
- <sup>34</sup>Key Laboratory of Cenozoic Geology and Environment, Institute of Geology and Geophysics, Chinese Academy of Sciences, No. 19 Beitucheng West Rd, Beijing, 100029, China
- <sup>35</sup>Departamento de Estratigrafía y Paleontología, Facultad de Ciencias, Universidad de Granada, Avda. Fuente Nueva S/N, 18002 Granada, Spain
- <sup>36</sup>Department of Geosciences and Geography, University of Helsinki, P.O. Box 64, 00014, Helsinki, Finland
- <sup>37</sup>Faculty of Geographical and Geological Sciences, Adam Mickiewicz University Poznań, Bogumiła Krygowskiego 10, 61-680 Poznań, Poland
- <sup>38</sup>Département de géographie, Université Laval, Québec City, QC, G1V 0A6, Canada
- <sup>39</sup>International Center for Climate and Environment Sciences, Institute of Atmospheric Physics, Chinese Academy of Sciences, Beijing, 100029, China
- <sup>40</sup>Shaanxi Key Laboratory of Earth Surface System and Environmental Carrying Capacity, College of Urban and Environmental Sciences, Northwest University, Xi'an 710127, China
- <sup>41</sup>Department of Geology, Tallinn University of Technology, Ehitajate tee 5, 19086 Tallinn, Estonia
- <sup>42</sup>Russian State Agrarian University, Timiryazevskaya St., 49, 127550, Moscow, Russia
- <sup>43</sup>Environmental Archaeology Research Group, Institute of History, CSIC, 28037 Madrid, Spain
- <sup>44</sup>ELKH-MTM-ELTE Research Group for Paleontology, Department of Environmental and Landscape Geography, Eötvös Loránd university, Pazmany Peter stny 1/c, 1117 Budapest, Hungary
- <sup>45</sup>Department of Geology, University of Latvia, Jelgavas iela 1, Riga, 1004, Latvia
- <sup>46</sup>Laboratory for Archaeobotany, State Office for Cultural Heritage Baden-Württemberg, Fischersteig 9, 78343 Gaienhofen-Hemmenhofen, Germany
- <sup>47</sup>Yale School of the Environment, New Haven, CT 06511, USA
- <sup>48</sup>Department of Geography, University of Nevada, Reno, 1664 N Virginia St., Reno, NV 89557, USA
- <sup>49</sup>Institute of Geological Sciences, Polish Academy of Sciences, Twarda 51/55, 00-818 Warsaw, Poland

- <sup>50</sup>Marlboro Institute for Liberal Arts and Interdisciplinary Studies, Emerson College, Boston, MA 02116, USA
- <sup>51</sup>Department of Geography, Urban and Regional Planning, University of Cantabria, 39005 Santander, Spain
- <sup>52</sup>Unitat de Botànica, Facultat de Biociències, Universitat Autònoma de Barcelona, Cerdanyola del Vallès, 08193 Barcelona, Spain
- <sup>53</sup>Ecosystems, Environment Research Programme, Environmental Change Research Unit (ECRU), Faculty of Biological and Environmental Sciences, University of Helsinki, Viikinkaari 1, P.O. Box 65, 00014, Helsinki, Finland
- <sup>54</sup>Department of Physical Geography and Ecosystem Science, Lund University, Lund, Sweden
- <sup>55</sup>Institut für Geographie, Universität Augsburg, 86135 Augsburg, Germany
- <sup>56</sup>Département de Géographie, Université de Montréal, Montréal, QC, H2V 0B3, Canada
- <sup>57</sup>Graduate School of Life and Environmental Sciences, Kyoto Prefectural University, Shimogamo, Sakyo-ku, 1-5 Hangi-cho, 606-8522 Kyoto, Japan
- <sup>58</sup>Institut für Geographie, Friedrich-Schiller-Universität Jena, Löbdergraben 32, 07743 Jena, Germany
- <sup>59</sup>Department of Renewable Resources, University of Alberta, 348B South Academic Building, Edmonton, AB, T6G 2H1, Canada
- <sup>60</sup>Institute of Geology and Geography, Nature Research Centre, Akademijos St. 2, 08412, Vilnius, Lithuania
- <sup>61</sup>Institute of Latvian History, University of Latvia, Kalpaka blv. 4, Riga, 1050, Latvia
- <sup>62</sup>Graduate School of Agriculture, Kyoto Prefectural University, Shimogamo, Sakyo-ku, 1-5, Hangi-cho, 606-8522 Kyoto, Japan
- <sup>63</sup>School of Environment and Chemistry Engineering, Xi'an Polytechnic University, Xi'an, Shaanxi 710048, China
- <sup>64</sup>Department of Biology, St Olaf College, 1520 St Olaf Ave, Northfield, MN 55057, USA
- <sup>65</sup>Department of Environmental Studies, St Olaf College, 1520 St Olaf Ave, Northfield, MN 55057, USA
- <sup>66</sup>State Key Laboratory of Lake Science and Environment, Nanjing Institute of Geography and Limnology, Chinese Academy of Sciences, Nanjing 210008, China
- <sup>67</sup>College of Resources and Environment Science, Hebei Normal University, Shijiazhuang 050024, China
- <sup>68</sup>Institute of Geographic Sciences and Natural Resources Research, Chinese Academy of Sciences, Beijing 100101, China

**Correspondence:** Sandy P. Harrison (s.p.harrison@reading.ac.uk)

Received: 12 August 2021 – Discussion started: 19 August 2021

Revised: 12 January 2022 – Accepted: 28 January 2022 – Published: 11 March 2022

**Abstract.** Sedimentary charcoal records are widely used to reconstruct regional changes in fire regimes through time in the geological past. Existing global compilations are not geographically comprehensive and do not provide consistent metadata for all sites. Furthermore, the age models provided for these records are not harmonised and many are based on older calibrations of the radiocarbon ages. These issues limit the use of existing compilations for research into past fire regimes. Here, we present an expanded database of charcoal records, accompanied by new age models based on recalibration of radiocarbon ages using IntCal20 and Bayesian age-modelling software. We document the structure and contents of the database, the construction of the age models, and the quality control measures applied. We also record the expansion of geographical coverage relative to previous charcoal compilations and the expansion of metadata that can be used to inform analyses. This first version of the Reading Palaeofire Database contains 1676 records (entities) from 1480 sites worldwide. The database (RPDv1b – Harrison et al., 2021) is available at <https://doi.org/10.17864/1947.000345>.

## 1 Introduction

Wildfires have major impacts on terrestrial ecosystems (Bond et al., 2005; Bowman et al., 2016; He et al., 2019; Lasslop et al., 2020), the global carbon cycle (Li et al., 2014; Arora and Melton, 2018; Pellegrini et al., 2018; Lasslop et al., 2019), atmospheric chemistry (van der Werf et al., 2010; Voulgarakis and Field, 2015; Sokolik et al., 2019), and climate (Randerson et al., 2006; Li et al., 2017; Harrison et al., 2018; Liu et al., 2019). Although the climatic, vegetation, and anthropogenic controls on wildfires are relatively well understood (e.g. Harrison et al., 2010; Bistinas et al., 2014; Knorr et al., 2016; Forkel et al., 2017; Li et al., 2019), recent years have seen wildfires occurring in regions where they were historically rare (e.g. northern Alaska, Greenland, northern Scandinavia – Evangeliou et al., 2019; Hayasaka, 2021) and an increase in fire frequency and severity in more fire-prone regions (e.g. California, the circum-Mediterranean, eastern Australia; e.g. Abatzoglou and Williams, 2016; Dutta et al., 2016; Williams et al., 2019; Nolan et al., 2020). It is useful to look at the pre-industrial era (conventionally defined as pre-1850 CE) to understand whether these events are atypical. The pre-industrial past also provides an opportunity to characterise fire regimes before anthropogenic influences, in terms of both ignitions and fire suppression, became important.

Ice-core records provide a global picture of changes in wildfire in the geologic past (Rubino et al., 2016). However, wildfires exhibit considerable local to regional variability because of the spatial heterogeneity of the various factors controlling their occurrence and intensity (Bistinas et al., 2014; Andela et al., 2019; Forkel et al., 2019). Thus, it is useful to use information that can provide a picture of regional changes through time. Charcoal, preserved in lake, peat, or marine sediments, can provide a picture of such changes (Clark and Patterson, 1997; Conedera et al., 2009). The wildfire regime can be characterised from sedimentary charcoal records through total charcoal abundance per unit of sediment, which can be considered a measure of the total biomass burned (e.g. Marlon et al., 2006), or by the presence of peaks in charcoal accumulation, which, in records with a sufficiently high temporal resolution, can indicate individual episodes of fire (e.g. Power et al., 2006).

The Global Paleofire Working Group (GPWG) was established in 2006 to coordinate the compilation and analysis of charcoal data globally, through the construction of the Global Charcoal Database (GCD – Power et al., 2008). The GPWG was initiated by the International Geosphere-Biosphere Programme (IGBP) Fast-Track Initiative on Fire and subsequently recognised as a working group of the Past Global Changes (PAGES) project in 2008. There have now been several iterations of the GCD (Power et al., 2008, 2010; Daniau et al., 2012; Blarquez et al., 2014; Marlon et al., 2016), which since 2020 has been managed by the International Paleofire Network as the Global Paleofire Database

(GPD; <https://paleofire.org>, last access: 21 February 2022). The GCD has been used to examine changes in fire regimes over the past 2 millennia (Marlon et al., 2008), during the current interglacial (Marlon et al., 2013), on glacial–interglacial timescales (Power et al., 2008; Daniau et al., 2012; Williams et al., 2015), and in response to rapid climate changes (Marlon et al., 2009; Daniau et al., 2010), as well as to examine regional fire histories (e.g. Mooney et al., 2011; Vanni ere et al., 2011; Marlon et al., 2012; Power et al., 2013a, b; Feurdean et al., 2020). However, there are a number of limitations to the use of the GCD for analyses of palaeofire regimes. Firstly, the database does not include many recently published records and needs to be updated. Secondly, there are inconsistencies among the various versions of the database including duplicated and/or missing sites, differences in the metadata included for each site or record, and missing metadata and dating information for some sites or records. Perhaps most crucially, the age models included in the database were made at different times, using different radiocarbon calibration curves, and using different age-modelling methods. The disparities between the archived age models preclude a detailed comparison of changes in wildfire regimes across regions.

Here, we present an expanded database of charcoal records (the Reading Palaeofire Database, RPD), accompanied by new age models based on recalibration of radiocarbon ages using IntCal20 (Reimer et al., 2020) and using a consistent Bayesian approach (Bacon – Blaauw et al., 2021) to age-model construction. However, we have retained the original age models for all the sites for comparison and to allow the user to choose a preferred age model. The RPD is designed to facilitate regional analyses of fire history; it is not designed as a permanent repository. We document the structure and contents of the database, the construction of the new age models, the expanded metadata available, and the quality control measures applied to check the data entry. We also document the expansion of the geographic and temporal coverage and the availability of metadata, relative to previous GCD compilations.

## 2 Data and methods

### 2.1 Compilation of data

The database contains sedimentary charcoal records, metadata to facilitate the interpretation of these records, and information on the dates used to construct the original age model for each record. Some records were obtained from the GCD. There are multiple versions of the GCD which differ in terms of the sites and the types of metadata included. We compared the GCDv3 (Marlon et al., 2016), GCDv4 (Blarquez, 2018), and GCD web page versions (<http://paleofire.org>, last access: 21 February 2022) and extracted a single unique version of each site and entity across the three versions. Where sites or entities were duplicated in different versions of the

GCD, we used the latest version. Missing metadata and dating information for these records were obtained from the literature or from the original data providers. Some sites in the GCD were represented by both concentration data and the same data expressed as influx (i.e. concentration per year) from the same samples; because influx calculations are time dependent, we have only retained concentration data for such sites to allow for future improvements to age models. Influx can be easily computed using data available in the RPD. We also removed duplicates where the GCD contained both raw data and concentration data from the same entity. We extracted published charcoal records from public repositories, specifically PANGAEA (<https://www.pangaea.de/>, last access: 21 February 2022), NOAA National Centers for Environmental Information (<https://www.ncdc.noaa.gov/data-access/paleoclimatology-data>, last access: 21 February 2022), the Neotoma Paleocology Database (<https://www.neotomadb.org/>, last access: 21 February 2022), the European Pollen Database (<http://www.europeanpollendatabase.net/index.php>, last access: 21 February 2022), and the Arctic Data Center (<https://arcticdata.io/catalog/>, last access: 21 February 2022); if these records were also in the GCD, we replaced the GCD version. Additional charcoal data, dating information, and metadata were provided directly by the authors. All the records in the current version of the database are listed in the Supplement (Table S1).

### 2.1.1 Structure of the database

The data are stored in a relational database (MySQL), which consists of 10 linked tables, specifically “site”, “entity”, “sample”, “date info”, “unit”, “entity link publication”, “publication”, “chronology”, “age model”, and “model name”. Figure 1 shows the relationships between these tables. A description of the structure and content of each of the tables is given below, and more detailed information about individual fields is given in the Supplement (Table S2).

### 2.1.2 Site metadata (table name – site)

A site is defined as the hydrological basin from which charcoal records have been obtained (Table 1). There may be several charcoal records from the same site, for example where charcoal records have been obtained on central and marginal cores from the same lake or where there is a lake core and additional cores from peatlands and/or terrestrial deposits (e.g. small hollows, soils) within the same hydrological basin. A site may therefore be linked to several charcoal records, where each record is treated as a separate entity. The site table contains basic metadata about the basin, including site ID, site name, latitude, longitude, elevation, site type, and maximum water depth. The site names are expressed without diacritics to facilitate database querying and subsequent analyses in programming languages that do not handle these characters. Latitude and longitude are given in decimal

degrees, truncated to six decimal places since this gives an accuracy of < 1 m at the Equator. Broad categories of site type are differentiated (e.g. terrestrial, lacustrine, marine), with subdivisions according to geomorphic origin (e.g. lakes are recorded according to whether they are, for example, fluvial, glacial, or volcanic in origin). In addition to coastal salt marshes and estuaries, we include a generic coastal category for all types of sites that lie within the coastal zone and whose hydrology may therefore have been affected by changes in sea level. Wherever possible, the size of the basin and the catchment are recorded (in km<sup>2</sup>), but if accurate quantified information is not available, the basin and catchment size are recorded by size classes. The site table also contains information on whether the lake or peatland is hydrologically closed or has inflows and outflows, which can affect the source, quantity, and preservation of charcoal in the sediments. A complete listing of the sites and entities in the RPD is given in Table S1. A list of the valid choices for fields that are selected from a pre-defined list (e.g. site type) is given in Table S2.

### 2.1.3 Entity metadata (table name – entity)

This table provides metadata for each individual entity (Table 2). In addition to distinguishing multiple cores from the same basin as separate entities, we also distinguish different size classes of charcoal from the same core when these data are available. Different charcoal size classes from the same core are also treated as separate entities in the database. However, we have removed duplicates where the same record was expressed in different ways (e.g. as both raw counts and concentration or as concentration and influx) to avoid confusion and mistakes when subsequently processing these data. The RPD contains raw data wherever possible and concentration data when the raw data are not available, and it only includes influx data if neither raw nor concentration data are available. When specific cores were given distinctive names in the original publication or by the original author, we include this information in the entity name for ease of cross-referencing. The entity metadata include information that can be used to interpret the charcoal records, including depositional context, core location, measurement method, and measurement unit. There is no standard measurement unit for charcoal, and in fact, there are > 100 different units employed in the database. For convenience, there is a link table to the measurement units (table name – unit). In addition, the entity table provides the source from which the charcoal data were obtained, including whether these data are from a version of the GCD or a data repository or were provided by the original author, and an indication of when the record was last updated. A list of the valid choices for fields that are selected from a pre-defined list (e.g. depositional context) is given in Table S2. A list of the charcoal measurement units currently in use in the RPD is given in Table S3.

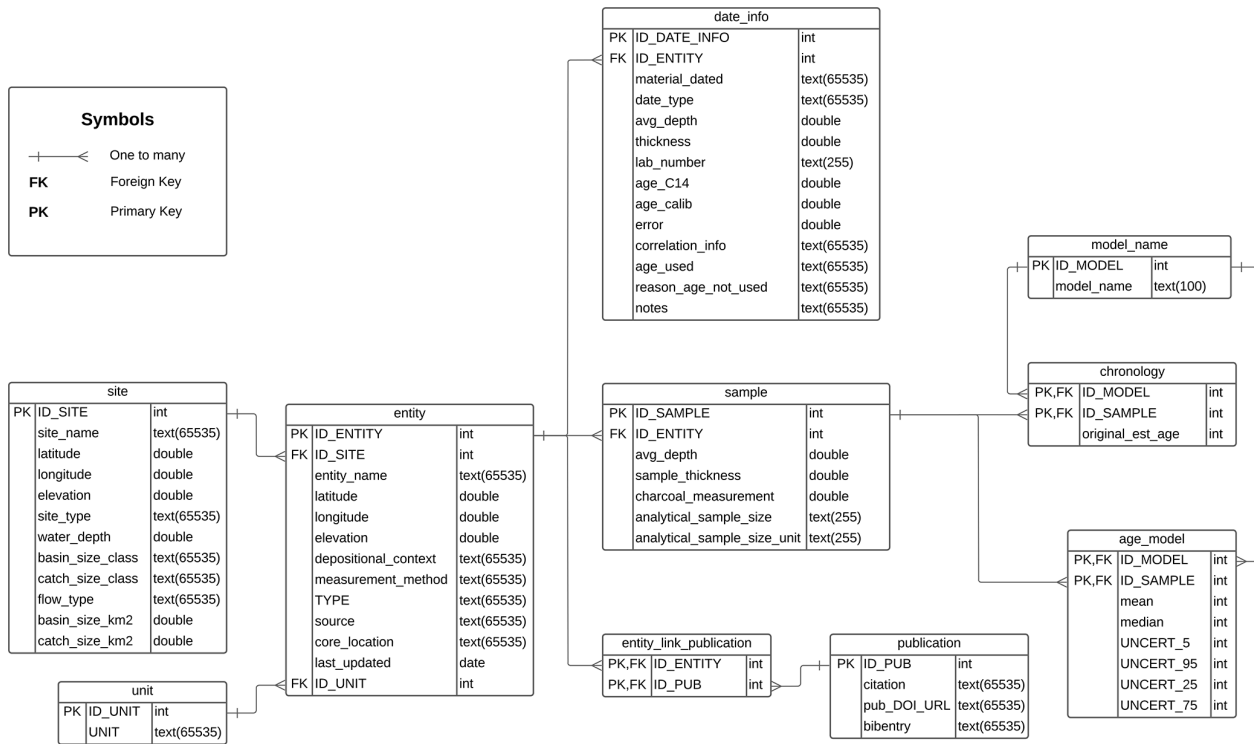


**Figure 1.** Diagram showing the structure of the database, individual tables and their contents, and the nature of the relationships between the component tables. One-to-many linkages indicate that it is possible to have several entries in one table linked to a single entry in another table. The database uses both primary and foreign keys. The primary key ensures that data included in a specific field are unique. The foreign key refers to the field in a table which is the primary key of another table and ensures that there is a link between these tables.

#### 2.1.4 Sample metadata and data (table name – sample)

The sample table provides information on the average depth in the core or profile and the thickness of the sample on which charcoal was measured (Table 3). The thickness measurements relate to the total thickness of the charcoal sample and provide an indication of whether the sampling was contiguous downcore. The sample table also provides information on the sample size and units and the quantity of charcoal present. The charcoal measurement units have been standardised by converting units expressed as multiples (e.g. fragments  $\times 100$ ) back to the whole numbers and by converting units expressed in milligrams or kilograms to grams. As a result, the values in the RPD may apparently differ from published values.

#### 2.1.5 Dating information (table name – date\_info)

This table provides information about the dates available for each entity that can be used to construct an age model (Table 4). We include information about the age of the core top for records that were known to be actively accumulating sediment at the time of collection. In addition to radiometric dates, we include information about the presence of tephtras (either dated at the site or independently dated elsewhere) and stratigraphic events that can be used to establish correla-

tive ages (e.g. changes in the pollen assemblage that are dated in other cores from the region or evidence of known fires in the catchment). Wherever possible the name of a tephra is given to facilitate the use of subsequent and more accurate estimates of its age. Similarly, the basis for correlative dates is given, again to facilitate the use of updated estimates of the age of the event. Radiocarbon ages are given in radiocarbon years, but all other ages are given in calendar years before present (BP) using 1950 CE as the reference zero date. Error estimates are given for radiometric ages and wherever possible for calendar ages. We provide an indication of whether a specific date was used in the original age model for the entity and an explanation for why specific dates were rejected, since this can be a guide as to whether the dates should be incorporated in the construction of new age models. A list of the valid choices for fields that are selected from a pre-defined list (e.g. material dated) is given in Table S2.

#### 2.1.6 Publication information (table name – publication)

This table provides full bibliographic citations for the original references documenting the charcoal records and/or their age models. There may be multiple publications for a single charcoal record, and all of these references are listed. Conversely, there may be a single publication for multiple

**Table 1.** Definition of the site table.

Field name	Definition	Data type	Constraints/notes
ID_SITE	Unique identifier for each site	Unsigned integer	Positive integer
site_name	Site name as given by original authors or as defined by us where there was no unique name given to the site	Text	Required
latitude	Latitude of the sampling site, given in decimal degrees, where N is positive and S is negative	Double	Numeric value between $-90$ and $90$
longitude	Longitude of the sampling site in decimal degrees, where E is positive and W is negative	Double	Numeric value between $-180$ and $180$
elevation	Elevation of the sampling site in metres above (+) or below (–) sea level	Double	None
site_type	Information about the type of site (e.g. lake, peatland, terrestrial)	Text	Selected from pre-defined list
water_depth	Water depth of the sampling site in metres	Double	None
flow_type	Indication of whether there is inflow and/or outflow from the sampled site	Text	Selected from pre-defined list
basin_size_km2	Size of sampled site (e.g. lake or bog) in $\text{km}^2$	Double	None
catch_size_km2	Size of hydrological catchment in $\text{km}^2$	Double	None
basin_size_class	Categorical estimate of basin size	Text	Selected from pre-defined list
catch_size_class	Categorical estimate of hydrological catchment size	Text	Selected from pre-defined list

charcoal records. There is also a table (table name – entity\_link\_publication) that links the publications to the specific entity.

### 2.1.7 Original age-model information (table name – chronology)

This table provides information about the original age model for each record and the ages assigned to individual samples. There can be many records that use the same type of age model (e.g. linear interpolation, spline, regression), and for convenience, there is a table that links the records to the age-model name (table name – model\_name).

### 2.1.8 New age-model information (table name – age\_model)

This table contains information about the age models that have been constructed for this version of the database using the IntCal20 calibration curve (Reimer et al., 2020) and the Bacon (Blaauw et al., 2021) age-modelling R package (see Sect. 2.3) (Table 5). We preserve information on the mean and median ages, as well as the quantile ranges for each sample.

## 2.2 Construction of new age models

The original age models for the charcoal records were made at different times, using different radiocarbon calibration curves, and using different age-modelling methods. We standardised the age modelling, using rbacon (Blaauw and Christen, 2011; Blaauw et al., 2021) to construct new Bayesian age–depth models in the ageR package (Villegas-Diaz et al., 2021). The ageR package provides functions that facilitate the supervised creation of multiple age models for many cores and different data sources, including databases and comma- and tab-separated files. The IntCal20 Northern Hemisphere calibration curve (Reimer et al., 2020) and the SHCal20 Southern Hemisphere calibration curve (Hogg et al., 2020) were used for entities between the latitudes of  $90$  and  $15^\circ$  N and  $15$  to  $90^\circ$  S respectively. Entities in equatorial latitudes ( $15^\circ$  N to  $15^\circ$  S) used a 50 : 50 mixed calibration curve to account for north–south air mass mixing following Hogg et al. (2020), and radiocarbon ages from marine entities were calibrated using the Marine20 calibration curve (Heaton et al., 2020).

To estimate the optimum age-modelling scenarios based upon the date and sample information for each entity, multiple rbacon age models were run using different prior accumulation rate (acc.mean) and thickness values. Prior accumulation rate values were selected using an initial linear regression of the ages in each entity, which was then increased



**Table 2.** Definition of the entity table.

Field name	Definition	Data type	Constraints/notes
ID_ENTITY	Unique identifier for each entity	Unsigned integer	Positive integer
ID_SITE	Refers to unique identifier for each site (as given in site table)	Unsigned integer	Auto-numeric, foreign key of the site table, a positive integer
entity_name	Name of entity, where an entity may be a separate core from the site or a separate type of measurement on the same core	Text	Required
latitude	Latitude of the entity, given in decimal degrees, where N is positive and S is negative	Double	A numeric value between $-90$ and $90$
longitude	Longitude of the entity, given in decimal degrees, where E is positive and W is negative	Double	A numeric value between $-180$ and $180$
elevation	Elevation of the sampling site, in metres above (+) or below (–) sea level	Double	None
depositional_context	Type of sediment sampled for charcoal	Text	Selected from pre-defined list
measurement_method	Method used to measure the amount of charcoal	Text	Selected from pre-defined list
TYPE	The unit type of the measured charcoal values (e.g. concentration, influx)	Text	Selected from pre-defined list
source	Source of charcoal data	Text	Selected from pre-defined list
core_location	Location of the entity within the site (e.g. central core or marginal core)	Text	Selected from pre-defined list
last_updated	Date when the entity or its linked data were last updated	Date	In format YYYY/mm/dd
ID_UNIT	Unique identifier for measurement unit (as in unit table)	Unsigned integer	Auto-numeric, foreign key of the unit table, a positive integer

**Table 3.** Definition of the sample table.

Field name	Definition	Data type	Constraints/notes
ID_SAMPLE	Unique identifier for each charcoal sample	Unsigned integer	Auto-numeric, primary key, a positive integer
ID_ENTITY	Unique identifier for the entity (as in entity table)	Unsigned integer	Auto-numeric, foreign key of the entity table, a positive integer
avg_depth	Average sampling depth, in metres	Double	None
sample_thickness	Sample thickness, in metres	Double	None
charcoal_measurement	Quantity of charcoal measured in the sample	Double	None
analytical_sample_size	Total amount of sediment sampled	Text	255-character maximum length
analytical_sample_size_unit	Units used for the sampling	Text	255-character maximum length

(decreased) sequentially from the default value to up to two times more (less) than the initial value. As an example, if the initial accumulation rate value selected from the linear regression was  $20 \text{ yr cm}^{-1}$ , age models would also be run using values of 10, 15, 20, 30, and  $40 \text{ yr cm}^{-1}$ . In cases where the

regional accumulation rate was known, the upper and lower values of the accumulation rate scenarios were manually constrained. The range of prior thicknesses used in the models was calculated by increasing and decreasing the rbacon default thickness value (5 cm) to up to a value one-eighth of the

**Table 4.** Definition of the date info table.

Field name	Definition	Data type	Constraints/notes
ID_DATE_INFO	Unique identifier for the date record	Unsigned integer	Auto-numeric, primary key, a positive integer
ID_ENTITY	Unique identifier for the entity (as in entity table)	Unsigned integer	Auto-numeric, foreign key of the entity table, a positive integer
material_dated	Material from which the date was obtained if applicable	Text	Selected from pre-defined list
date_type	Technique used to obtain the date measurement	Text	Selected from pre-defined list
avg_depth	Average depth in the sedimentary sequence where the date was measured, in metres	Double	None
thickness	Thickness of the sample used for dating, in metres	Double	None
lab_number	Unique identifying code assigned by the dating laboratory	Text	65 535-character maximum length
age_C14	Uncalibrated radiocarbon age	Double	None
age_calib	The calendar age of a date	Double	None
error	Analytical or measurement error of the date	Double	None
correlation_info	Indication of basis for correlative dating (e.g. pollen, tephra, or stratigraphic correlations)	Text	Selected from pre-defined list
age_used	Indicates whether date was used by the author(s) in the construction of the original age model	Text	Selected from pre-defined list
reason_age_not_used	Indication of why a date was not used in the original age model, blank if dates were used in original model	Text	Selected from pre-defined list
notes	Additional comments regarding a date record	Text	65 535-character maximum length

overall length of the core. For a 400 cm core for example, the thickness scenarios would be 5, 10, 15, 20, 25, 30, 35, 40, 45, and 50 cm. Thus, the number of scenarios created by possible accumulation rates and thicknesses varies between different entities. Depths of known hiatuses reported in the original publications were included in the date\_info table (Sect. 2.1.5) and have also been included in the age models run in ageR. In instances where the sedimentation rates were different above and below a hiatus, separate age models were run before and after the non-deposition period to account for these variations (Blaauw and Christen, 2011).

A three-step procedure was used to select the best model for each entity. First, an optimum model was selected by ageR, using the lowest quantified area between the prior and posterior accumulation rate distribution curves (Supplement Fig. S1). This selection was checked manually using comparisons between the distance of the estimated ages and the controls to check the accuracy of the model interpolation.

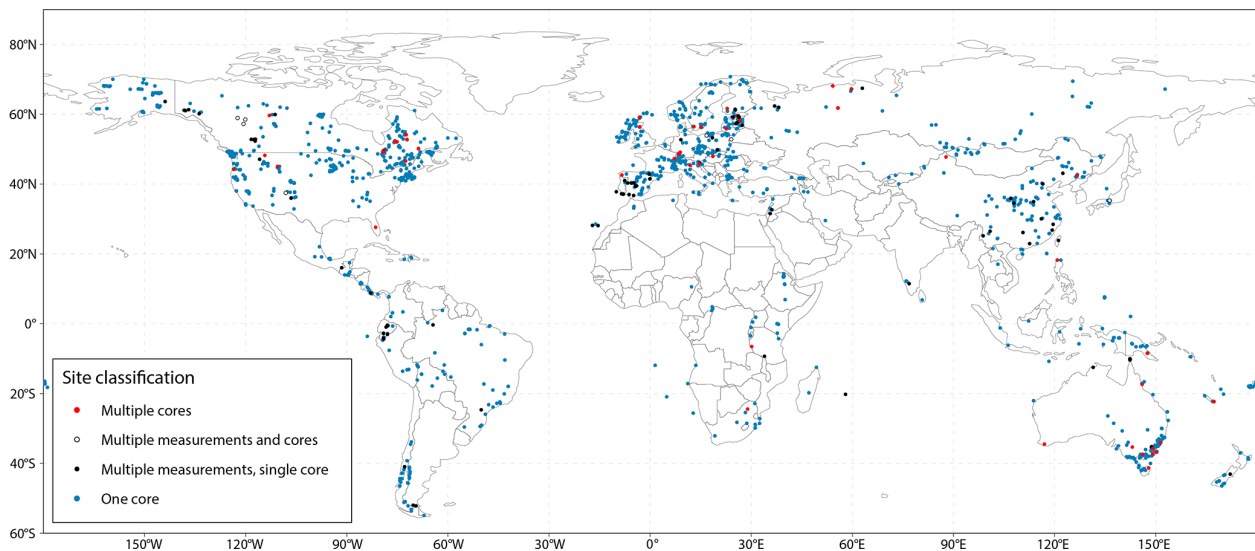
Finally, the age model was visually inspected to ensure that final interpolation accurately represented the date information and did not show abrupt shifts in accumulation rates or changes at the dated depths. If the ageR model selection was deemed to be erroneous or inaccurate, the next suitable model with the lowest area between the prior and posterior curves, which accurately represented the distribution of dates in the sequence, was selected (Supplement Fig. S2).

### 2.3 Quality control

Individual records in the RPD were compiled either by the original authors or from published and open-access material by specialists in the collection and interpretation of charcoal records. Records that were obtained from published and open-access material were cross-checked against publications or with the original authors of those publications whenever possible. Null values for metadata fields were identified

**Table 5.** Definition of the age-model table.

Field name	Definition	Data type	Constraints/notes
ID_MODEL	Unique identifier for the technique used to generate the age model (original age models from existing authors in the chronology table and new age models in the age_model table)	Unsigned integer	Auto-numeric, composite primary key with ID_SAMPLE, foreign key of the model_name table, positive integer
ID_SAMPLE	Unique identifier for the sample (as in sample table)	Unsigned integer	Auto-numeric, composite primary key with ID_MODEL, foreign key of the sample table, positive integer
mean	Mean age of the sample	Integer	None
median	Median age of the sample	Integer	None
UNCERT_5	Lower bound of the 95 % confidence interval for the median age	Integer	None
UNCERT_95	Upper bound of the 95 % confidence interval for the median age	Integer	None
UNCERT_25	Lower bound of the 75 % confidence interval for the median age	Integer	None
UNCERT_75	Upper bound of the 75 % confidence interval for the median age	Integer	None

**Figure 2.** Map showing the location of sites included in the RPD. As shown here, some sites have multiple records, either representing separate cores from the same hydrological basin or representing measurements of different charcoal size fractions on the same core. These records are treated as separate entities in the database itself.

during the initial checking procedure, and checks were made with the data contributors to determine whether these genuinely corresponded to missing information. In the database, null values are reserved for fields where the required information is not applicable, for example water depth for terrestrial sites or laboratory sample numbers for correlative dates. We distinguish fields where information could be available

but was never recorded or has subsequently been lost (represented by  $-999999$ ) and fields where we were unable to obtain this information but it could be included in subsequent updates of the database (represented by  $-777777$ ). We also distinguish fields where specific metadata are not applicable (represented by  $-888888$ ), for example basin size for a marine core or water depth for a terrestrial small hollow.

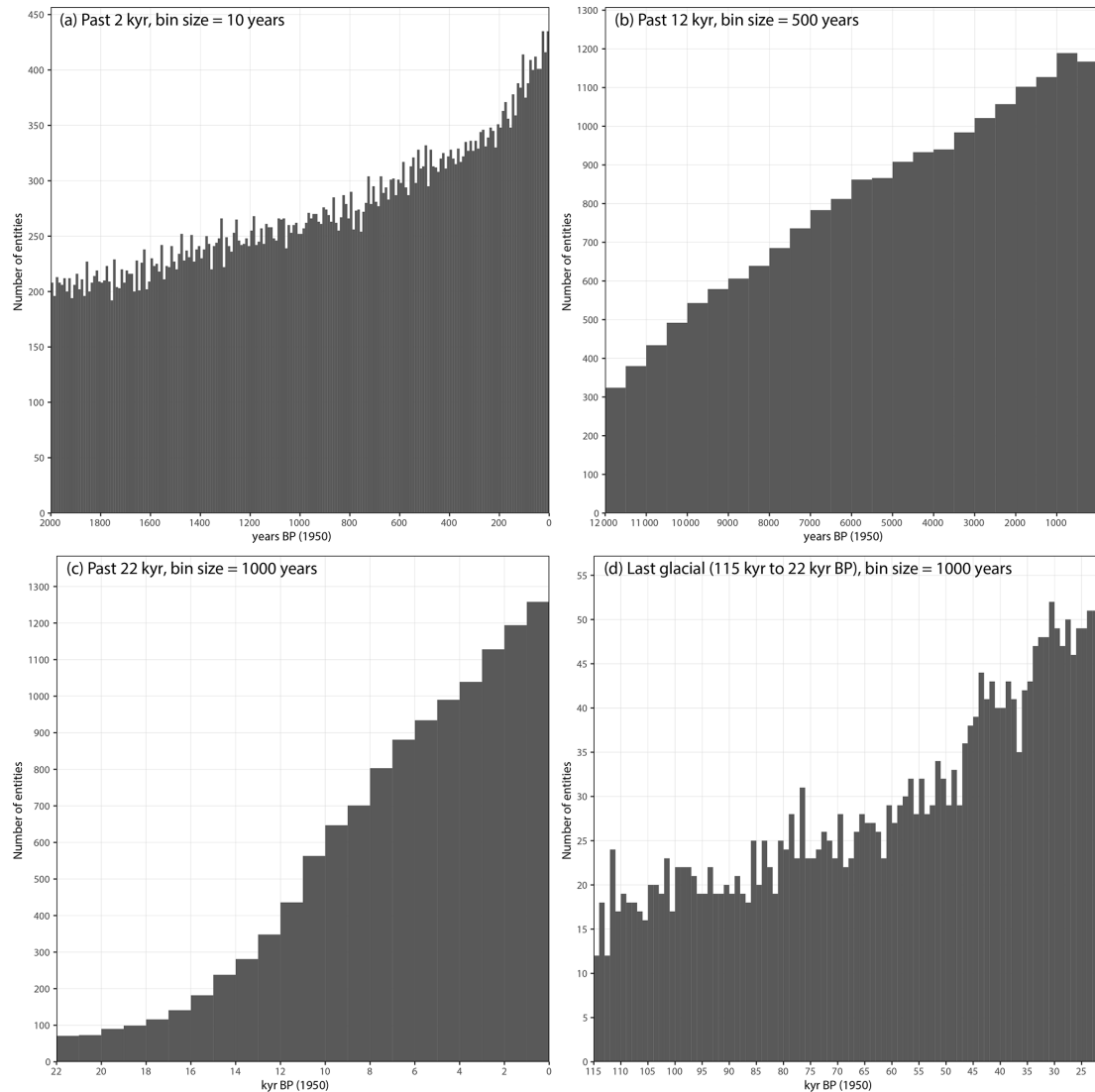


**Figure 3.** Plots showing the temporal coverage of individual entities in the database. Panel (a) shows records covering the past 2000 years (2 kyr BP); panel (b) shows records covering the past 12 000 years (12 kyr BP); panel (c) shows records for the past 22 000 years (22 kyr BP), thus encompassing the Last Glacial Maximum (LGM); panel (d) shows records that cover the interval of the last glacial prior to the LGM (22–115 kyr BP).

Prior to entry in the database, the records were automatically checked using specially designed database scripts (in R) to ensure that the entries to individual fields were in the format expected (e.g. text, decimal numeric, positive integers) or were selected from the pre-defined lists provided for specific fields. Checks were also performed to find duplicated rows (e.g. duplicated sampling depths within the same entity).

### 3 Overview of database contents

This first version of the RPD contains 1676 individual charcoal records from 1480 sites worldwide. This represents a 128 % increase compared to the number of records in ver-

sion 3 of the Global Charcoal Database (GCDv3; Marlon et al., 2016; 736 records), a 79 % increase compared to version 4 (Blarquez, 2018; 935 records), and a 36 % increase compared to the online version of the GCD (1232 records). The RPD includes 840 records that are not available in any version of the GCD and provides updated or corrected information for a further 485 records that were included in the GCD. Raw data are available for 14 % of the entities and concentration for 67 % of the entities; influx based on the original age models is given for 16 % of the entities. The original age models for 67 (4 %) of the records included in the RPD were derived solely by layer counting, U–Th or Pb dates, or isotopic correlation and therefore are already expressed in calendar ages. However, we have provided new age models

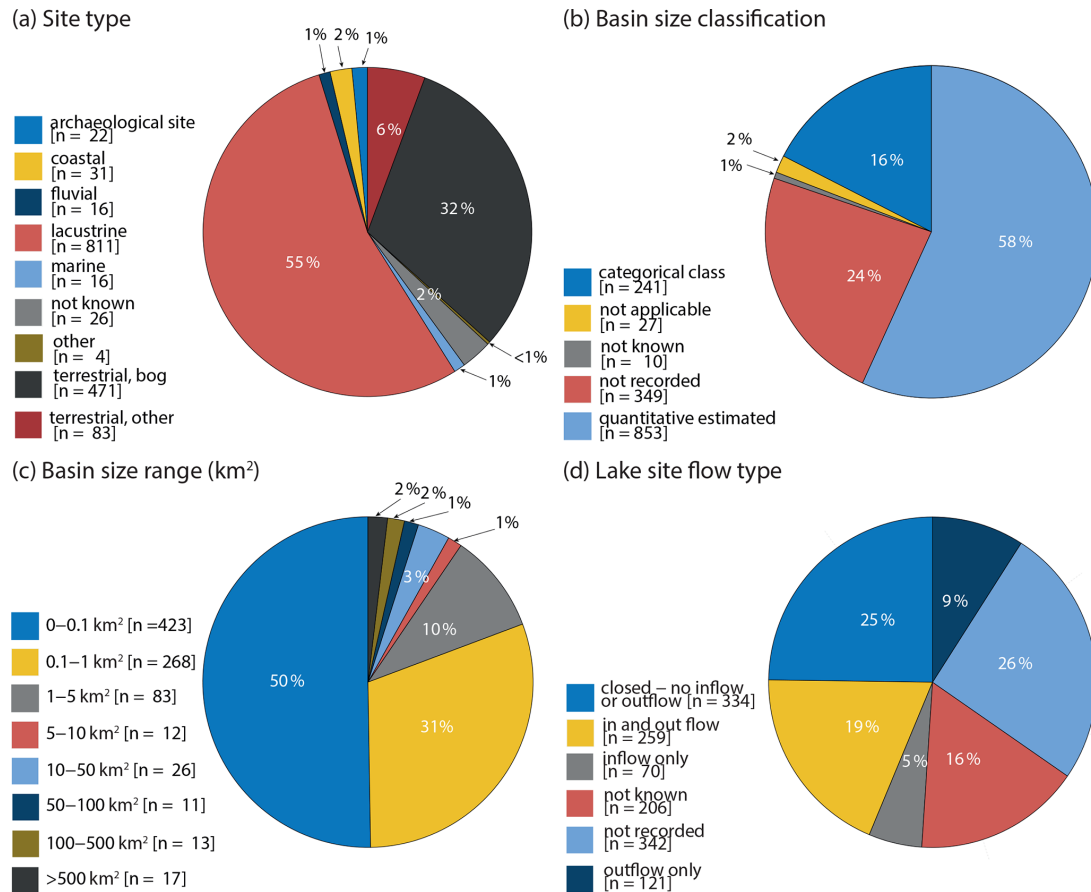


**Figure 4.** Availability of metadata that can be used to select suitable sites for specific analyses or for quality control. Plot (a) shows the distribution of sites by type. Some site types have finer distinctions recorded in the database: lacustrine environments, for example, are subdivided according to origin. Plot (b) shows the number of sites with quantitative estimates versus categorical assessments of basin size, and plot (c) shows the number of sites in specific basin size ranges. Plot (d) shows the distribution of different hydrological types for lake records.

for 22 of these records (33 %), where the dates or correlation points were specified, using the supervised age-modelling procedure for consistency. New age models have been created for 807 (50 %) of the remaining charcoal records where the original chronology was based on radiometric dating. The geographic coverage of the RPD (Fig. 2) is biased towards the northern extratropics. However, there is a growing representation of records from China, the neotropics (Central and South America), southern and eastern Africa, and eastern Australia. The largest gaps geographically are in currently dry regions, which often lack sites with anoxic sedimentation suitable for the preservation of charcoal and are generally under-represented in palaeofire reconstructions (Leys et al., 2018). The temporal coverage of the records is excellent for the interval starting 22 000 years ago, with 774 records with a minimum resolution of 10 years for the past 2000 years, 1335 records with a minimum resolution of 500 years for the past 12 000 years, and 1382 records with a minimum resolution of 1000 years for the past 22 000 years (Fig. 3).

There are fewer records for earlier intervals. Nevertheless, there are 70 records that provide evidence for the interval of the last glacial period before the Last Glacial Maximum (22–115 ka) including the response of fire to rapid climate warming (Dansgaard–Oeschger events).

Information about site type (Fig. 4a) is included in the database because this could influence whether the charcoal is of local origin or represents a more regional palaeofire signal. For example, records from small forest hollows provide a very local signal of fire activity and records from peat bogs most likely sample fires on the peatland itself, whereas records from lakes could provide both local and regional fire signals. More than half (55 %) of the records in the RPD are derived from lakes (811 entities). Records from peatlands are also well represented (471 entities, 32 %). Basin size, particularly in the case of lakes, influences the source area for charcoal particles transported by wind. However, the existence of inflows and outflows to the system can also affect the charcoal record. Quantitative information is now avail-

able for more than half of the lake sites (Fig. 4b), and most (691 sites, 81 %) of the records (Fig. 4c) are from relatively small lakes (< 1 km<sup>2</sup>). A quarter of the charcoal records from lakes (Fig. 4d) are from closed basins (334 sites).

#### 4 Data availability

Version 1 of the Reading Palaeofire Database (RPDv1b – Harrison et al., 2021) is available in SQL format at <https://doi.org/10.17864/1947.000345>. The individual tables are also available as .csv files. The R package used to create the new age models is available at <https://github.com/special-uor/ageR> (last access: 21 February 2022) and <https://doi.org/10.5281/zenodo.4636716> (Villegas-Diaz et al., 2021).

#### 5 Conclusions

The Reading Palaeofire Database (RPD) is an effort to improve the coverage of charcoal records that can be used to investigate palaeofire regimes. New age models have been developed for 48 % of the records to take account of recent improvements in radiocarbon calibration and age-modelling methods. In addition to expanded coverage and improved age models, considerable effort has been made to include metadata and quality control information to allow the selection of records appropriate to address specific questions and to document potential sources of uncertainty in the interpretation of the records. The first version of the RPD contains 1676 individual charcoal records (entities) from 1480 sites worldwide. Geographic coverage is best for the northern extratropics, but the coverage is good overall except for in semi-arid and arid regions. Temporal coverage is good for the past 2000 years, the Holocene, and back to the LGM, but there are a reasonable number of longer records. The database is publicly available, both as an SQL database and as .csv files.

**Supplement.** The supplement related to this article is available online at: <https://doi.org/10.5194/essd-14-1109-2022-supplement>.

**Author contributions.** SPH and RVD designed the database; RVD, DK, PL, and SPH were responsible for construction of the database; ALD advised on incorporation of data from the GCD and the standardisation of charcoal units; ECS, DG, DK, PL, YS, and LS provided updated age models; the other authors provided original data or metadata and quality control on individual records; SPH wrote the first draft of the paper, and all authors contributed to the final draft.

**Competing interests.** The contact author has declared that neither they nor their co-authors have any competing interests.

**Disclaimer.** Publisher's note: Copernicus Publications remains neutral with regard to jurisdictional claims in published maps and institutional affiliations.

**Acknowledgements.** Roberto Villegas-Diaz, Sandy P. Harrison, Esmeralda Cruz-Silva, and Yicheng Shen acknowledge support from the ERC-funded project GC2.0 (Global Change 2.0: Unlocking the past for a clearer future, grant number 694481). Sandy P. Harrison, Paul Lincoln, Daniel Gallagher, David Kesner, and Luke Sweeney acknowledge support from the Leverhulme Centre for Wildfires, Environment and Society through the Leverhulme Trust, grant number RC-2018-023. Angelica Feurdean acknowledges support from the German Research Foundation (grant no. FE-1096/6-1). Katarzyna Marcisz acknowledges support from the Swiss Government Excellence Postdoctoral Scholarship (grant no. FIRECO 2016.0310); the National Science Centre in Poland (grant no. 2015/17/B/ST10/01656); grant PSPB-013/2010 from Switzerland through the Swiss contribution to the enlarged European Union; and the Scientific Exchange Programme from the Swiss Contribution to the New Member States of the European Union and Switzerland (Sciex-NMSch) – SCIEX Scholarship Fund, project RE-FIRE 12.286. Olga Lisitsyna acknowledges support from the Mobilitas Plus post-doctoral research grant of the Estonian Research Council (MOBJD313). We would like to thank our many colleagues from the PAGES Global Paleofire Working Group for their contributions to the construction of the Global Charcoal Database, which provided the starting point for the current compilation, and our colleagues from the Leverhulme Centre for Wildfires, Environment and Society for discussions on the use of palaeodata to reconstruct past fire regimes. We thank Manfred Rösch for providing information on dating for several sites. We also thank Dan Gavin and Jack Williams for helpful reviews of the original manuscript.

**Financial support.** This research has been supported by the Leverhulme Trust (grant no. RC-2018-023), the European Research Council (grant no. 694481), the German Research Foundation (grant no. FE-1096/6-1), the Swiss Government Excellence Postdoctoral Scholarships (grant no. FIRECO 2016.0310), the National Science Centre of Poland (grant no. 2015/17/B/ST10/01656), the SCIEX Scholarship Fund (grant no. PSPB-013/2010), and the Estonian Research Council (grant no. MOBJD313).

**Review statement.** This paper was edited by David Carlson and reviewed by Daniel Gavin and one anonymous referee.

#### References

- Abatzoglou, J. T., and Williams, A. P.: Impact of anthropogenic climate change on wildfire across western US forests, *P. Natl. Acad. Sci. USA*, 113, 11770–11775, <https://doi.org/10.1073/pnas.1607171113>, 2016.
- Andela, N., Morton, D. C., Giglio, L., Paugam, R., Chen, Y., Hantson, S., van der Werf, G. R., and Randerson, J. T.: The Global Fire Atlas of individual fire size, duration,

- speed and direction, *Earth Syst. Sci. Data*, 11, 529–552, <https://doi.org/10.5194/essd-11-529-2019>, 2019.
- Arora, V. K. and Melton, J. R.: Reduction in global area burned and wildfire emissions since 1930s enhances carbon uptake by land, *Nat. Commun.*, 9, 1326, <https://doi.org/10.1038/s41467-018-03838-0>, 2018.
- Bistinas, I., Harrison, S. P., Prentice, I. C., and Pereira, J. M. C.: Causal relationships versus emergent patterns in the global controls of fire frequency, *Biogeosciences*, 11, 5087–5101, <https://doi.org/10.5194/bg-11-5087-2014>, 2014.
- Blaauw, M., Christen, J. A., Aquino Lopez, M. A., Esquivel Vazquez, J., Gonzalez, O. M., Belding, T., Theiler, J., Gough, B., and Karney, C.: rbacon: Age-Depth Modelling using Bayesian Statistics, <https://CRAN.R-project.org/package=rbacon> (last access: 21 February 2022), 2021.
- Blaauw, M. J. and Christen, A.: Flexible paleoclimate age-depth models using an autoregressive gamma process, *Bayesian Anal.*, 6, 457–474, <https://doi.org/10.1214/11-BA618>, 2011.
- Blarquez, O.: GCD, <https://CRAN.R-project.org/package=GCD> (last access: 21 February 2022), 2018.
- Blarquez, O., Vanni re, B., Marlon, J. R., Daniau, A.-L., Power, M. J., Brewer, S., and Bartlein, P. J.: paleofire: An R package to analyse sedimentary charcoal records from the Global Charcoal Database to reconstruct past biomass burning, *Comput. Geosci.*, 72, 255–261, <https://doi.org/10.1016/j.cageo.2014.07.020>, 2014.
- Bond, W. J., Woodward, F. I., and Midgley, G. F.: The global distribution of ecosystems in a world without fire, *New Phytol.*, 165, 525–538, 2005.
- Bowman, D. M. J. S., Perry, G. L. W., Higgins, S. I., Johnson, C. N., Fuhlendorf, S. D., and Murphy, B. P.: Pyrodiversity is the coupling of biodiversity and fire regimes in food webs, *Philos. T. R. Soc. Lond.*, 371, 20150169, <https://doi.org/10.1098/rstb.2015.0169>, 2016.
- Clark, J. S. and Patterson, W. A.: Background and local charcoal in sediments: Scales of fire evidence in the paleo-record, in: *Sediment Records of Biomass Burning and Global Change*, Springer Berlin Heidelberg, Berlin, Heidelberg, 23–48, [https://doi.org/10.1007/978-3-642-59171-6\\_3](https://doi.org/10.1007/978-3-642-59171-6_3), 1997.
- Conedera, M., Tinner, W., Neff, C., Meurer, M., Dickens, A. F., and Krebs, P.: Reconstructing past fire regimes: methods, applications, and relevance to fire management and conservation, *Quaternary Sci. Rev.*, 28, 555–576, <https://doi.org/10.1016/j.quascirev.2008.11.005>, 2009.
- Daniau, A.-L., Harrison, S. P., and Bartlein, P. J.: Fire regimes during the last glacial, *Quaternary Sci. Rev.*, 29, 2918–2930, 2010.
- Daniau, A.-L., Bartlein, P. J., Harrison, S. P., Prentice, I. C., Brewer, S., Friedlingstein, P., Harrison-Prentice, T. I., Inoue, J., Marlon, J. R., Mooney, S., Power, M. J., Stevenson, J., Tinner, W., Andri , M., Atanassova, J., Behling, H., Black, M., Blarquez, O., Brown, K. J., Carcaillet, C., Colhoun, E., Colombaroli, D., Davis, B. A. S., D’Costa, D., Dodson, J., Dupont, L., Eshetu, Z., Gavin, D. G., Genries, A., Gebru, T., Haberle, S., Hallett, D. J., Horn, S., Hope, G., Katamura, F., Kennedy, L., Kershaw, P., Krivonogov, S., Long, C., Magri, D., Marinova, E., McKenzie, G. M., Moreno, P. I., Moss, P., Neumann, F. H., Norstr m, E., Paitre, C., Rius, D., Roberts, N., Robinson, G., Sasaki, N., Scott, L., Takahara, H., Terwilliger, V., Thevenon, F., Turner, R. B., Valsecchi, V. G., Vanni re, B., Walsh, M., Williams, N., and Zhang, Y.: Predictability of biomass burning in response to climate changes, *Global Biogeochem. Cy.*, 26, GB4007, <https://doi.org/10.1029/2011GB004249>, 2012.
- Dutta, R., Das, A., and Aryal, J.: Big data integration shows Australian bush-fire frequency is increasing significantly, *Royal Society Open Science*, 3, 150241, <https://doi.org/10.1098/rsos.150241>, 2016.
- Evangelio, N., Kylling, A., Eckhardt, S., Myroniuk, V., Stebel, K., Paugam, R., Zibitsev, S., and St hl, A.: Open fires in Greenland in summer 2017: transport, deposition and radiative effects of BC, OC and BrC emissions, *Atmos. Chem. Phys.*, 19, 1393–1411, <https://doi.org/10.5194/acp-19-1393-2019>, 2019.
- Feurdean, A., Vanni re, B., Finsinger, W., Warren, D., Connor, S. C., Forrest, M., Liakka, J., Panait, A., Werner, C., Andri , M., Bobek, P., Carter, V. A., Davis, B., Diaconu, A.-C., Dietze, E., Feeser, I., Florescu, G., Ga ka, M., Giesecke, T., Jahns, S., Jamrichov, E., Kajuka o, K., Kaplan, J., Karpi nska-Ko aczek, M., Ko aczek, P., Kune , P., Kupriyanov, D., Lamentowicz, M., Lemmen, C., Magyari, E. K., Marcisz, K., Marinova, E., Nimamir, A., Novenko, E., Obremaska, M., P dziszewska, A., Pfeiffer, M., Poska, A., R sch, M., S lowi nski, M., Stan ikait , M., Szal, M.,  wi ta-Musznicka, J., Tan u, I., Theuerkauf, M., Tonkov, S., Valk , O., Vassiljev, J., Veski, S., Vincze, I., Wacnik, A., Wiethold, J., and Hickler, T.: Fire hazard modulation by long-term dynamics in land cover and dominant forest type in eastern and central Europe, *Biogeosciences*, 17, 1213–1230, <https://doi.org/10.5194/bg-17-1213-2020>, 2020.
- Forkel, M., Dorigo, W., Lasslop, G., Teubner, I., Chuvieco, E., and Thonicke, K.: A data-driven approach to identify controls on global fire activity from satellite and climate observations (SOFIA V1), *Geosci. Model Dev.*, 10, 4443–4476, <https://doi.org/10.5194/gmd-10-4443-2017>, 2017.
- Forkel, M., Andela, N., Harrison, S. P., Lasslop, G., van Marle, M., Chuvieco, E., Dorigo, W., Forrest, M., Hantson, S., Heil, A., Li, F., Melton, J., Sitch, S., Yue, C., and Arneeth, A.: Emergent relationships with respect to burned area in global satellite observations and fire-enabled vegetation models, *Biogeosciences*, 16, 57–76, <https://doi.org/10.5194/bg-16-57-2019>, 2019.
- Harrison, S. P., Marlon, J. R., and Bartlein, P. J.: Fire in the Earth System, in: *Changing Climates, Earth Systems and Society International Year of Planet Earth*, Springer Publisher, 21–48, 2010.
- Harrison, S. P., Bartlein, P. J., Brovkin, V., Houweling, S., Kloster, S., and Prentice, I. C.: The biomass burning contribution to climate–carbon-cycle feedback, *Earth Syst. Dynam.*, 9, 663–677, <https://doi.org/10.5194/esd-9-663-2018>, 2018.
- Harrison, S. P., Villegas-Diaz, R., Lincoln, P., Kesner, D., Cruz-Silva, E., Sweeney, L., Shen, Y., and Gallagher, D.: The Reading Palaeofire Database: an expanded global resource to document changes in fire regimes from sedimentary charcoal records, University of Reading [data set], <https://doi.org/10.17864/1947.319>, 2021.
- Hayasaka, H.: Rare and extreme wildland fire in Sakha in 2021, *Atmosphere*, 1, 1572, <https://doi.org/10.3390/atmos12121572>, 2021.
- He, T., Lamont, B. B., and Pausas, J. G.: Fire as a key driver of Earth’s biodiversity, *Biol. Rev.*, 94, 1983–2010, <https://doi.org/10.1111/brv.12544>, 2019.
- Heaton, T., K hler, P., Butzin, M., Bard, E., Reimer, R., Austin, W., Bronk Ramsey, C., Grootes, P. M., Highen, K. A., Kromer, B., Reimer, P. J., Adkins, A., Burke, A. M., Cook, M. S., Olsen,

- J., and Skinner, L.: Marine 20 – The marine radiocarbon age calibration curve (0–55,000 cal BP), *Radiocarbon*, 62, 779–820, <https://doi.org/10.1017/RDC.2020.68>, 2020.
- Hogg, A., Heaton, T., Hua, Q., Palmer, J., Turney, C., Southon, J., Bayliss, A., Blackwell, P. G., Boswijk, G., Bronk Ramsey, C., Pearson, C., Petchey, F., Reimer, P., Reimer, R., and Wacker, L.: SHCal 20 southern Hemisphere calibration, 0–55,000 years cal BP, *Radiocarbon*, 62, 759–778, <https://doi.org/10.1017/RDC.2020.59>, 2020.
- Knorr, W., Jiang, L., and Arneeth, A.: Climate, CO<sub>2</sub> and human population impacts on global wildfire emissions, *Biogeosciences*, 13, 267–282, <https://doi.org/10.5194/bg-13-267-2016>, 2016.
- Lasslop, G., Coppola, A. I., Voulgarakis, A., Yue, C., and Veraverbeke, S.: Influence of fire on the carbon cycle and climate, *Curr. Clim. Change Rep.*, 5, 112–123, <https://doi.org/10.1007/s40641-019-00128-9>, 2019.
- Lasslop, G., Hantson, S., Harrison, S. P., Bachelet, D., Burton, C., Forkel, M., Forrest, M., Li, F., Melton, J. R., Yue, C., Archibald, S., Scheiter, S., Arneeth, A., Hickler, T., and Sitch, S.: Global ecosystems and fire: multi-model assessment of fire-induced tree cover and carbon storage reduction, *Glob. Change Biol.*, 26, 5027–5041, <https://doi.org/10.1111/gcb.15160>, 2020.
- Leys, B., Marlon, J. R., Umbanhowar, C., and Vanniere, B.: Global fire history of grassland biomes, *Ecol. Evolut.*, 8, 8831–8852, 2018.
- Li, F., Bond-Lamberty, B., and Levis, S.: Quantifying the role of fire in the Earth system – Part 2: Impact on the net carbon balance of global terrestrial ecosystems for the 20th century, *Biogeosciences*, 11, 1345–1360, <https://doi.org/10.5194/bg-11-1345-2014>, 2014.
- Li, F., Lawrence, D. M., and Bond-Lamberty, B.: Impact of fire on global land surface air temperature and energy budget for the 20th century due to changes within ecosystems, *Environ. Res. Lett.*, 12, 044014, <https://doi.org/10.1088/1748-9326/aa6685>, 2017.
- Li, F., Val Martin, M., Andreae, M. O., Arneeth, A., Hantson, S., Kaiser, J. W., Lasslop, G., Yue, C., Bachelet, D., Forrest, M., Kluzek, E., Liu, X., Mangeon, S., Melton, J. R., Ward, D. S., Darmanov, A., Hickler, T., Ichoku, C., Magi, B. I., Sitch, S., van der Werf, G. R., Wiedinmyer, C., and Rabin, S. S.: Historical (1700–2012) global multi-model estimates of the fire emissions from the Fire Modeling Intercomparison Project (FireMIP), *Atmos. Chem. Phys.*, 19, 12545–12567, <https://doi.org/10.5194/acp-19-12545-2019>, 2019.
- Liu, Z., Ballantyne, A. P., and Cooper, L. A.: Biophysical feedback of global forest fires on surface temperature, *Nat. Commun.*, 10, 214, <https://doi.org/10.1038/s41467-018-08237-z>, 2019.
- Marlon, J., Bartlein, P. J., and Whitlock, C.: Fire-fuel-climate linkages in the northwestern USA during the Holocene, *Holocene*, 16, 1059–1071, 2006.
- Marlon, J., Bartlein, P. J., Carcaillet, C., Gavin, D. G., Harrison, S. P., Higuera, P. E., Joos, F., Power, M., and Prentice, I. C.: Climate and human influences on global biomass burning over the past two millennia, *Nat. Geosci.*, 1, 697–702, <https://doi.org/10.1038/ngeo313>, 2008.
- Marlon, J. R., Bartlein, P. J., Walsh, M. K., Harrison, S. P., Brown, K. J., Edwards, M. E., Higuera, P. E., Power, M. J., Anderson, R. S., Briles, C., Brunelle, A., Carcaillet, C., Daniels, M., Hu, F. S., Lavoie, M., Long, C., Minckley, T., Richard, P. J. H., Scott, A. C., Shafer, D. S., Tinner, W., Umbanhower Jr., C. E., and Whitlock, C.: Wildfire responses to abrupt climate change in North America, *P. Natl. Acad. Sci. USA*, 106, 2519–2524, <https://doi.org/10.1073/pnas.0808212106>, 2009.
- Marlon, J. R., Bartlein, P. J., Long, C., Gavin, D. G., Anderson, R. S., Briles, C., Brown, K., Colombaroli, D., Hallett, D. J., Power, M. J., Scharf, E., and Walsh, M. K.: Long-term perspective on wildfires in the western U.S.A., *P. Natl. Acad. Sci. USA*, 109, E535–E543, <https://doi.org/10.1073/pnas.1112839109>, 2012.
- Marlon, J. R., Bartlein, P. J., Daniau, A.-L., Harrison, S. P., Power, M. J., Tinner, W., Maezumie, S., and Vannière, B.: Global biomass burning: A synthesis and review of Holocene paleofire records and their controls, *Quaternary Sci. Rev.*, 65, 5–25, 2013.
- Marlon, J. R., Kelly, R., Daniau, A.-L., Vannière, B., Power, M. J., Bartlein, P., Higuera, P., Blarquez, O., Brewer, S., Brücher, T., Feurdean, A., Romera, G. G., Iglesias, V., Maezumi, S. Y., Magi, B., Courtney Mustaphi, C. J., and Zhihai, T.: Reconstructions of biomass burning from sediment-charcoal records to improve data–model comparisons, *Biogeosciences*, 13, 3225–3244, <https://doi.org/10.5194/bg-13-3225-2016>, 2016.
- Mooney, S., Harrison, S. P., Bartlein, P. J., Daniau A.-L., Stevenson, J., Brownlie, K., Buckman, S., Cupper, M., Luly, J., Black, M., Colhoun, E., D’Costa, D., Dodson, J., Haberle, S., Hope, G. S., Kershaw, P., Kenyon, C., McKenzie, M., and Williams, N.: Late Quaternary fire regimes of Australasia, *Quaternary Sci. Rev.*, 30, 28–46, 2011.
- Nolan, R. H., Boer, M. M., Collins, L., Resco de Dios, V., Clarke, H., Jenkins, M., Kenny, B., and Bradstock, R. A.: Causes and consequences of eastern Australia’s 2019–20 season of mega-fires, *Glob. Change Biol.*, 26, 1039–1041, <https://doi.org/10.1111/gcb.14987>, 2020.
- Pellegrini, A. F. A., Ahlström, A., Hobbie, S. E., Reich, P. B., Nieradzki, L. P., Staver, A. C., Scharenbroch, B. C., Jumpponen, A., William R. L. Anderegg, W. R. L., James T. Randerson, J. T., and Jackson, R. B.: Fire frequency drives decadal changes in soil carbon and nitrogen and ecosystem productivity, *Nature*, 553, 194–198, <https://doi.org/10.1038/nature24668>, 2018.
- Power, M. J., Whitlock, C., Bartlein, P. J., and Stevens, L.R.: Fire and vegetation history during the last 3800 years in northwestern Montana, *Geomorphology*, 75, 420–436, 2006.
- Power, M. J., Ortiz, N., Marlon, J., Bartlein, P. J., Harrison, S. P., Mayle, F., Ballouche, A., Bradshaw, R., Carcaillet, C., Cordova, C., Mooney, S., Moreno, P., Prentice, I. C., Thonicke, K., Tinner, W., Whitlock, C., Zhang, Y., Zhao, Y., Anderson, R. S., Beer, R., Behling, H., Briles, C., Brown, K., Brunelle A., Bush, M., Clark, J., Colombaroli, D., Chu, C. Q., Daniels, M., Dodson, J., Edwards, M. E., Fisinger, W., Gavin, D. G., Gobet, E., Hallett, D. J., Higuera, P., Horn, S., Inoue, J., Kaltenrieder, P., Kennedy, L., Kong, Z. C., Long, C., Lynch, J., Lynch, B., McGlone, M., Meeks, S., Meyer, G., Minckley, T., Mohr, J., Noti, R., Pierce, J., Richard, P., Shuman, B. J., Takahara, H., Toney, J., Turney, C., Umbanhower, C., Vandergoes, M., Vanniere, B., Vescovi, E., Walsh, M., Wang, X., Williams, N., Wilmshurst, J., and Zhang, J. H.: Changes in fire activity since the LGM: an assessment based on a global synthesis and analysis of charcoal data, *Clim. Dynam.*, 30, 887–907, <https://doi.org/10.1007/s00382.00.0334x>, 2008.



- Power, M. J., Marlon, J. R., Bartlein, P. J., and Harrison, S. P.: Fire history and the Global Charcoal Database: a new tool for hypothesis testing and data exploration, *Palaeogeogr. Palaeoclim.*, 291, 52–59, <https://doi.org/10.1016/j.palaeo.2009.09.014>, 2010.
- Power, M. J., Mayle, F. E., Bartlein, P. J., Marlon, J. R., Anderson, R. S., Behling, H., Brown, K. J., Carcaillet, C., Colombaroli, D., Gavin, D. G., Hallett, D. J., Horn, S. P., Kennedy, L. M., Lane, C. S., Long, C. J., Moreno, P. I., Paitre, C., Robinson, G., Taylor, Z., and Walsh, M. K.: 16th Century burning decline in the Americas: population collapse or climate change?, *Holocene*, 23, 3–13, <https://doi.org/10.1177/0959683612450196>, 2013a.
- Power, M. J., Mayle, F., Bartlein, P., Marlon, J. R., Anderson, R. S., Behling, H., Brown, K. J., Carcaillet, C., Colombaroli, D., Gavin, D. G., Hallett, D. J., Horn, S. P., Kennedy, L. M., Lane, C. S., Long, C. J., Moreno, P. I., Paitre, C., Robinson, G., Taylor, Z., and Walsh, M. K.: Climatic control of the biomass-burning decline in the Americas after ad 1500, *Holocene*, 23, 3–13, <https://doi.org/10.1177/0959683612450196>, 2013b.
- Randerson, J. T., Liu, H., Flanner, M. G., Chambers, S. D., Jin, Y., Hess, P. G., Pfister, G., Mack, M. C., Treseder, K. K., Welp, L. R., Chapin, F. S., Hardeb, J. W., Goulden, M. L., Lyons, E., Neff, J. C., Schuur, E. A. G., and Zender, C. S.: The impact of boreal forest fire on climate warming, *Science*, 314, 1130–1132, 2006.
- Reimer, P., Austin, W., Bard, E., Bayliss, A., Blackwell, P., Bronk Ramsey, C., Butzin, M., Cheng, H., Edwards, R. L., Friedrich, M., Grootes, P. M., Guilderson, T. P., Hajdas, I., Heaton, T. J., Hogg, A. G., Hughen, K. A., Kromer, B., Manning, S. W., Muscheler, R., Palmer, J. G., Pearson, C., van der Plicht, J., Reimer, R. W., Richards, D. A., Scott, E. M., Southon, J. R., Turney, C. S. M., Wacker, L., Adolphi, F., Buntgen, U., Capano, M., Fahrni, S. M., Fogtmann-Schulz, A., Friedrich, R., Kohler, P., Kudsk, S., Miyake, F., Olsen, J., Reinig, F., Sakamoto, M., Sookdeo, M., and Talamo, S.: The IntCal20 Northern Hemisphere radiocarbon age calibration curve (0–55 calkBP), *Radiocarbon*, 62, 725–757, <https://doi.org/10.1017/RDC.2020.41>, 2020.
- Rubino, M., D’Onofrio, A., Seki, O., and Bendle, J. A.: Ice-core records of biomass burning, *Anthrop. Rev.*, 3, 140–162, <https://doi.org/10.1177/2053019615605117>, 2016.
- Sokolik, I. N., Soja, A. J., DeMott, P. J., and Winker, D.: Progress and challenges in quantifying wildfire smoke emissions, their properties, transport, and atmospheric impacts. *J. Geophys. Res.-Atmos.*, 124, 13005–12025, <https://doi.org/10.1029/2018JD029878>, 2019.
- van der Werf, G. R., Randerson, J. T., Giglio, L., Collatz, G. J., Mu, M., Kasibhatla, P. S., Morton, D. C., DeFries, R. S., Jin, Y., and van Leeuwen, T. T.: Global fire emissions and the contribution of deforestation, savanna, forest, agricultural, and peat fires (1997–2009), *Atmos. Chem. Phys.*, 10, 11707–11735, <https://doi.org/10.5194/acp-10-11707-2010>, 2010.
- Vannière, B., Power, M. J., Roberts, N., Tinner, W., Carrión, J., Magny, M., Bartlein, P. J., and GPWG contributors: Circum-Mediterranean fire activity and climate changes during the mid Holocene environmental transition (8500–2500 cal yr BP), *Holocene*, 21, 53–73, 2011.
- Villegas-Diaz, R., Cruz-Silva, E., and Harrison, S. P.: ageR: Supervised Age Models, Zenodo [code], <https://doi.org/10.5281/zenodo.4636716>, 2021.
- Voulgarakis, A. and Field, R. D. Fire influences on atmospheric composition, air quality and climate, *Curr. Pollution Rep.*, 1, 70–81, <https://doi.org/10.1007/s40726-015-0007-z>, 2015.
- Williams, A. N., Mooney, S. D., Sisson, S. A., and Marlon, J. R.: Exploring the relationship between Aboriginal population indices and fire in Australia over the last 20,000 years, *Palaeogeogr. Palaeoclim.*, 432, 49–57, 2015.
- Williams, A. P., Abatzoglou, J. T., Gershunov, A., Guzman-Morales, J., Bishop, D. A., Balch, J. K., and Lettenmaier, D. P.: Observed impacts of anthropogenic climate change on wildfire in California, *Earth’s Future*, 7, 892–910, <https://doi.org/10.1029/2019EF001210>, 2019.